JOC Article
pubs.acs.org/joc

Versatile Strategy To Access Fully Functionalized Benzodifurans: Redox-Active Chromophores for the Construction of Extended π-Conjugated Materials

Chenyi Yi,[†] Carmen Blum,[†] Mario Lehmann,[†] Stephan Keller,[†] Shi-Xia Liu,*[,†] Gabriela Frei,[†] Antonia Neels,[‡] Jürg Hauser,[†] Stefan Schürch,[†] and Silvio Decurtins[†]

[†]*Departement für Chemie und Biochemie, Universität Bern, Freiestrasse 3, CH-3012 Bern, Switzerland, and* [‡]*XRD Application LAB, CSEM Centre Suisse d'Electronique et de Microtechnique SA, Jaquet-Droz 1, Case postale, CH-2002 Neuchâtel, Switzerland*

liu@iac.unibe.ch

Received March 1, 2010

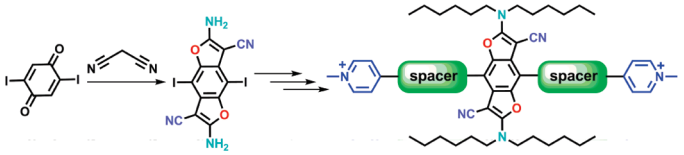

An efficient synthetic approach to construct a fully substituted benzo[1,2-*b*:4,5-*b*′]difuran (BDF) **2a** via base-catalyzed double annulations is presented. Compound **2a** can readily undergo Suzuki, Heck, and Sonogashira coupling reactions to afford in good yields a manifold of extended π-conjugated BDF derivatives, e.g., with pyridine termini (**4**−**6**) and with different spacers. These are highly luminescent materials that undergo two reversible one-electron oxidations. Remarkably, their photophysical and electrochemical properties can be largely tuned by methylation or protonation. Consequently, they can function as pH-dependent fluorescence switches. Finally, the observed electronic properties are explained on the basis of density functional theory.

Introduction

Derivatives of the heterocyclic compounds benzofuran and benzodifuran (BDF) are ubiquitous in nature, and they show a wide range of pharmacological properties and biological activities which consequently put them into the focus of longstanding and widespread interest in the fields of bioorganic and medical research.[1]

Additionally, within the field of materials chemistry, BDF derivatives proved also to be excellent compounds for high-performance hole-transporting materials,[2] which, for instance, find applications in multilayer organic light-emitting diodes (OLEDs), organic field-effect transistors (OFETs), and photovoltaic cells. Specifically, the synergetic effect of the BDF core and the different substituents which extend the π-conjugation of the BDF skeleton play a decisive role; this is an issue which is directly relevant in the context of the present work. This class of planar and highly conjugated heterocyclic molecules can also be addressed as organic fluorophores[3] which classifies them, altogether, as multifunctional materials. However, only quite limited reports on their synthesis appear in the literature. A common approach involves the intramolecular double-cyclization formation of a difuran moiety starting from properly substituted arenes.[4] For example, various multisubstituted BDFs have been

(1) (a) Chambers, J. J.; Kurrasch-Orbaugh, D. M.; Parker, M. A.; Nichols, D. E. *J. Med. Chem.* **2001**, *44*, 1003. (b) Chambers, J. J.; Kurrasch-Orbaugh, D. M.; Nichols, D. E. *Bioorg. Med. Chem. Lett.* **2002**, *12*, 1997. (c) Verghese, J.; Liang, A.; Sidhu, P. P. S.; Hindle, M.; Zhou, Q.; Desai, U. R. *Bioorg. Med. Chem. Lett.* **2009**, *19*, 4126. (d) Kim, I.; Choi, J. *Org. Biomol. Chem.* **2009**, *7*, 2788. (e) Manna, K.; Agrawal, Y. K. *Bioorg. Med. Chem. Lett.* **2009**, *19*, 2688. (f) De Luca, L; Nieddu, G.; Porcheddu, A.; Giacomelli, G. *Curr. Med. Chem.* **2009**, *16*, 1. (g) Liang, Z.; Ma, S.; Yu, J.; Xu, R. *Tetrahedron* **2007**, *63*, 12877.

(2) Tsuji, H.; Mitsui, C.; Ilies, L.; Sato, Y.; Nakamura, E. *J. Am. Chem. Soc.* **2007**, *129*, 11902.

(3) (a) Hayashi, N; Saito, Y.; Higuchi, H.; Suzuki, K. *J. Phys. Chem. A* **2009**, *113*, 5342. (b) Baraldi, I.; Benassi, E.; Ciorba, S.; Sindler-Kulyk, M.; Skoric, I.; Spalletti, A. *Chem. Phys.* **2009**, *361*, 61.

(4) (a) Liang, Z.; Ma, S.; Yu, J.; Xu, R. *J. Org. Chem.* **2007**, *72*, 9219. (b) Quezada, E.; Delogu, G.; Vina, D.; Santana, L.; Podda, G.; Matos, M. J.; Picciau, C. *Helv. Chim. Acta* **2009**, *92*, 1309. (c) Caruso, U.; Panunzi, B.; Roviello, G. N.; Roviello, G.; Tingoli, M.; Tuzi, A. *C. R. Chimie* **2009**, *12*, 622. (d) Davarani, S. S. H.; Fakhari, A. R.; Fumani, N. S.; Kalate-bojdi, M. *Electrochem. Commun.* **2008**, *10*, 1765. (e) Peltzmann, R.; Unterweger, B.; Junek, H. *Monatsh. Chem.* **1979**, *110*, 739.

Published on Web 04/26/2010 DOI: 10.1021/jo100323s

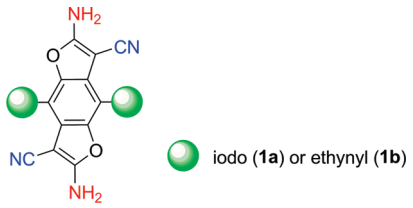

FIGURE 1. Chemical structure of the fully functionalized benzo-[1,2-*b*:4,5-*b*′]difuran (BDF) derivatives.

obtained in good yields by using palladium-catalyzed double annulations of bis(allyloxy)bis(alkynyl)benzenes or bis(alkynyl)-dihydroxybenzenes in the presence of allylic halides.[4a]

To create a novel series of molecules that could have potentially interesting material properties, we embarked on the design and synthesis of a range of fully functionalized BDFs. Herein, we report a facile and efficient synthetic protocol to a fully functionalized benzo[1,2-*b*:4,5-*b*′]difuran (BDF) molecule **1** (Figure 1). This approach has a number of advantages. First, two nitrile groups at the 3,7-positions of the BDF core substantially extend the π-conjugated BDF skeleton. Second, two amine functions located at the 2,6-positions, when alkylated, render good solubility and processability to the rigid backbone, which are prerequisite for the attainment of a variety of functional materials. Finally, the 1,4-positions of the benzene core are occupied either by an iodo functionality or by pending ethynyl groups, which clearly renders a motif for employing Suzuki, Heck, and Sonogashira coupling reactions to prepare a broad range of functional molecules. For example, the BDF derivatives **1** can act as precursors for the construction of oligo(*p*-phenyleneethylene) (OPE)[5]-type compounds which are of particular interest in organic molecular (opto)electronics.

It is well-known that molecules with pyridyl substituents at the terminal positions are expected to be alligator clips for the synthesis of molecular devices.[6] They can also afford interesting supramolecular architectures with fascinating properties by intermolecular interactions and coordination with metal ions.[7] In this context, three BDF derivatives **4**−**6** with pyridine termini and different spacers have been synthesized via the corresponding Suzuki, Heck, and Sonogashira coupling reactions of the key precursor **2a**, which can be obtained after hexylation of **1a**. Moreover, their dimethylated compounds **7**−**9** have been prepared as viologen analogues. Viologens have been widely used in the fundamental study of electrochemical, photoelectrochemical, and electrochromic materials[8] and solar energy conversion.[9]

Results and Discussion

Synthesis. Because of our interest in malononitrile chemistry,[10] we probed the reactivity of malononitrile with iodo- or ethynyl-substituted 1,4-benzoquinones (Schemes 1 and 2), demonstrating that multifunctionalized BDF molecules can be elaborated via a base-catalyzed intramolecular cyclization. We assume that a plausible reaction mechanism is analogous to the one proposed by Obushak et al.[11] This one-pot process involves a Michael reaction between the carbanion of malononitrile and quinone, followed by an intramolecular double cyclization. As shown in Scheme 1, **1a** is readily available from 2,5-diiodo-1,4-benzoquinone. However, it was observed that **1a** could not be converted into **1b** (shown in Scheme 2) through the Sonogashira coupling reaction, very probably because of its poor solubility.

We envisioned the same methodology as for **1a** to be applicable to the synthesis of **1b** (Scheme 2). Thus, 2,5-bis-(trimethylsilylethynyl)-1,4-benzoquinone was used, which can be prepared in excellent yield from 1,4-diiodo-2,5-dimethoxybenzene through a Sonogashira coupling and subsequent oxidation reaction. Under the reaction conditions of the final step, desilylation was concomitantly induced to give **1b** directly, but only in low yield. Seemingly, the trimethylsilylethynyl groups are unstable and interfere with the reaction process.

Next, Pd-catalyzed Sonogashira coupling reactions of **1a** with 4-ethynylpyridine and of **1b** with 4-iodopyridine have been tested. However, due to the poor solublility of these BDF compounds, the desired coupling products could not be isolated. In order to circumvent this problem, hexyl groups have been introduced to afford **2a** in satisfactory yield (Scheme 1). The synthesis of **2b** consists of Pd-catalyzed Sonogashira coupling and subsequent deprotection of the alkynes. Compound **2a** was readily converted into BDF derivatives **4**−**6** with pyridine termini via the Suzuki coupling with 4-pyridylboronic acid, the Sonogashira coupling with 4-ethynylpyridine, or the Heck coupling with 4-vinylpyridine (Scheme 3). Additionally, an alternative approach to **5** involving the Sonogashira coupling reaction of **2b** with 4-iodopyridine has been investigated, showing that with this protocol **5** can only be isolated in 29% yield (see the Supporting Information). The lower yield indicates that the self-coupling of alkynes takes place under the tested reaction conditions. Notably, as illustrated in Scheme 3, quaternization of the pyridine termini of **4**−**6** was performed by treatment with an excess of methyl iodide in CH_3CN under microwave irradiation to afford the corresponding conjugation-extended viologen derivatives **7**−**9** in good yields. All new compounds were unambiguously characterized by spectroscopic analyses and also by single-crystal X-ray analyses in the case of **1b** and **4**−**6**.

(5) (a) Dalton, G. T.; Cifuentes, M. P.; Watson, L. A.; Petrie, S.; Stranger, R.; Samoc, M.; Humphrey, M. G. *Inorg. Chem.* **2009**, *48*, 6534. (b) Tang, Y.; Zhou, Z.; Ogawa, K.; Lopez, G. P.; Schanze, K. S.; Whitten, D. G. *Langmuir* **2009**, *25*, 21. (c) Shi, Z.-F.; Wang, L.-J.; Wang, H.; Cao, X.-P.; Zhang, H.-L. *Org. Lett.* **2007**, *9*, 595. (d) Wang, C.; Batsanov, A. S.; Bryce, M. R.; Sage, I. *Org. Lett.* **2004**, *6*, 2181. (e) Hundt, N.; Palaniappan, K.; Servello, J.; Dei, D. K.; Stefan, M. C.; Biewer, M. C. *Org. Lett.* **2009**, *11*, 4422.

(6) Chantean, S. H.; Tour, J. M. *Tetrahedron Lett.* **2001**, *42*, 3057.

(7) (a) Zaman, M. B.; Tomura, M.; Yamashita, Y. *J. Org. Chem.* **2001**, *66*, 5987. (b) Biradha, K.; Hongo, Y.; Fujita, M. *Angew. Chem., Int. Ed.* **2000**, *39*, 3843. (c) Belanger, S.; Hupp, J. T.; Stern, C. L.; Slone, R. V.; Wastone, D. F.; Carrel, T. G. *J. Am. Chem. Soc.* **1999**, *121*, 557. (d) Miller, J. S.; Epstein, A. J. *Angew. Chem., Int. Ed. Engl.* **1994**, *33*, 385.

(8) (a) Bockman, M. T.; Kochi, K. J. *J. Org. Chem.* **1990**, *55*, 4127. (b) Barltrop, A. J.; Jackson, C. A. *J. Chem. Soc., Perkin Trans. 2* **1984**, 367. (c) Monk, P. M. S. *The viologens: Physicochemical Properties, Synthesis and Applications of the Salts of 4,4′-Bipyridine*; John Wiley & Sons Ltd.: Chichester, 1998.

(9) Vermeulen, A. L.; Thompson, E. M. *Nature* **1992**, *358*, 656.

(10) (a) Yi, C.; Blum, C.; Liu, S.-X.; Frei, G.; Neels, A.; Renaud, P.; Leutwyler, S.; Decurtins, S. *J. Org. Chem.* **2008**, *73*, 3596. (b) Yi, C.; Blum, C.; Liu, S.-X.; Frei, G.; Neels, A.; Stoeckli-Evans, H.; Leutwyler, S.; Decurtins, S. *Tetrahedron* **2008**, *64*, 9437. (c) Yi, C.; Blum, C.; Liu, S.-X.; Ran, Y.-F.; Frei, G.; Neels, A.; Stoeckli-Evans, H.; Calzaferri, G.; Leutwyler, S.; Decurtins, S. *Cryst. Growth Des.* **2008**, *8*, 3004.

(11) Obushak, M. D.; Martyak, R. L.; Matiychuk, V. S. *Pol. J. Chem.* **2002**, *76*, 1419.

SCHEME 1. Synthetic Routes to 2a and 2b

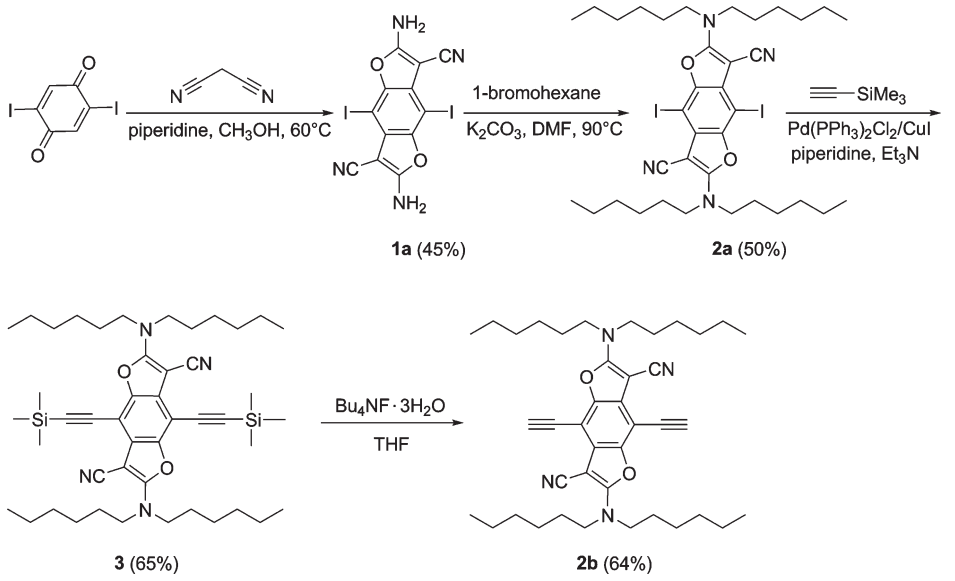

SCHEME 2. Synthetic Route to 1b

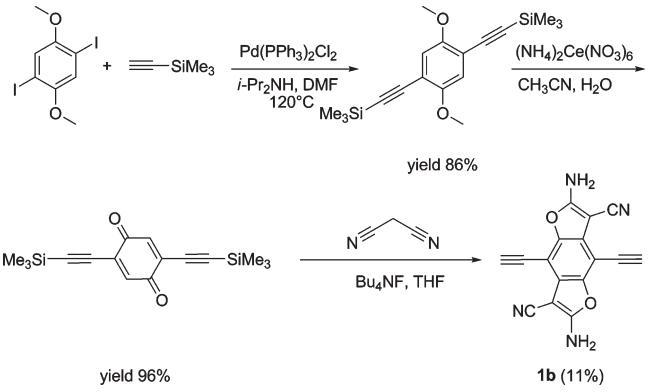

Structural Studies. Compound **5** crystallizes as solvate-free orange rods in the triclinic space group $P\bar{1}$, while compound **6** crystallizes as solvate-free orange needles in the monoclinic space group $P2_1/c$. In both cases, two crystallographically independent molecules (**A**, **B**) are found in the unit cell showing only small differences in their structural parameters; the crystallographic inversion center is located at the C_6 ring. The BDF core is nearly planar; the rms deviations from least-squares planes through the heterocyclic skeletons are 0.01 Å (**A**) and 0.22 Å (**B**) of compound **5** and 0.02 Å (**A** and **B**) for compound **6**, respectively. The dihedral angles formed between the pyridine rings and the BDF unit are 18.7(4)° and 21.5(5)° for **5** and 14.9(4)° and 16.0(4)° for **6**. There are no exceptional geometrical features, and all bond lengths and angles are within the expected range; they compare well with reported structures of BDF derivatives.[12,13] As an example, the molecular structure of **5** is shown in Figure 2 (Figure S6, Supporting Information for **6**).

In the crystal lattices (Figures S1 and S7, Supporting Information), the molecules are stacked along the *a*-axis (**5**) or the *b*-axis (**6**). Distinct molecular directions are twisted for adjacent molecules within the stacks by angles of ~70° (**5**) or ~90° (**6**). In the case of **5**, the stacking alignment is mainly caused by $\pi\cdots\pi$ interactions; the interplanar separations between the least-squares planes of the molecular cores amounts to 3.24(1) Å. In contrast, the molecular arrangement for **6** is mainly driven by van der Waals interactions between the aliphatic chains. Consequently, the interplanar distances are > 5 Å. The crystal structures and crystal packings of **1b** and **4** are shown in Figures S2−S3 and S4−S5 (Supporting Information), respectively. In contrast to the nearly planar structures of **5** and **6**, the compound **4** adopts a nonplanar conformation with a dihedral angle of 53.1(1)° between the pyridine rings and the BDF unit due to ortho-repulsive interactions between cyano groups and pyridine rings.

Electrochemistry. The electrochemical properties of **4**−**9** in CH_2Cl_2 were investigated by cyclic voltammetry (CV). Their electrochemical data are collected in Table 1, and Figure 3 exhibits as a typical example the CV curves for compound **6** and its viologen derivative **9**. All compounds undergo two well-separated and reversible single-electron oxidation processes to the BDF centered radical cation and dication states. Compared to molecules **4** and **6**, compound **5** exhibits high oxidation potentials, very probably because of the strong electron-withdrawing effect of the 4-pyridylethynyl groups. Note that, upon protonation or methylation, the oxidation potentials are significantly positive-shifted, which can be attributed to the significant electron-withdrawing effect of the pyridinium groups. In addition, the methylated BDF derivatives **7** and **9** show a reversible two-electron reduction peak suggesting that they behave as the π-extended viologens. Obviously, their cation radical states are thermodynamically unstable because of their nonplanar structures, which is in good agreement with previously published results.[14] Compound **9** shows a less negative reduction potential ($E_{1/2}$ = −0.67 V) than **7** ($E_{1/2}$ = −0.89 V) due to the

(12) Shukla, R.; Wadumethrige, S. H.; Lindeman, S. V.; Rathore, R. *Org. Lett*. **2008**, *10*, 3587.

(13) Choi, H. D.; Seo, P. J.; Son, B. W.; Lee, U. *Acta Crystallogr*. **2007**, *E63*, o2920.

(14) Takahashi, K.; Nihira, T.; Akiyama, K.; Ikegami, Y.; Fukuyo, E. *J. Chem. Soc., Chem. Commun*. **1992**, 620.

SCHEME 3. Synthetic Routes to Compounds 4−9

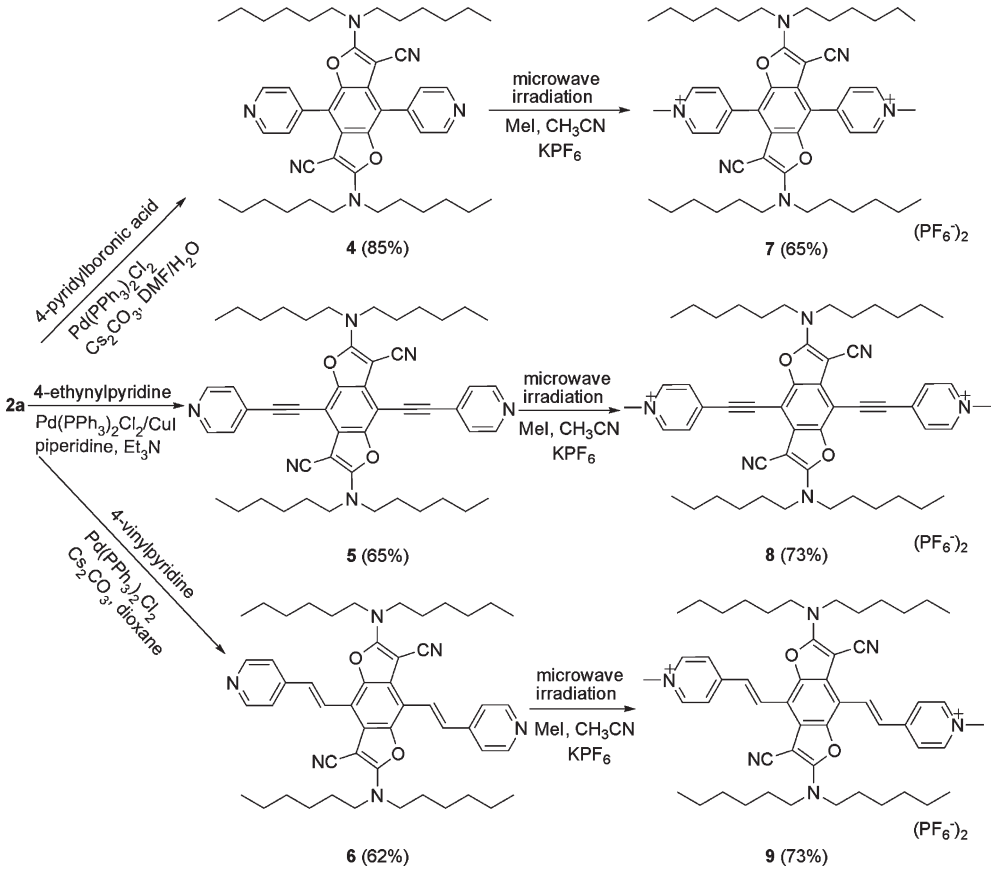

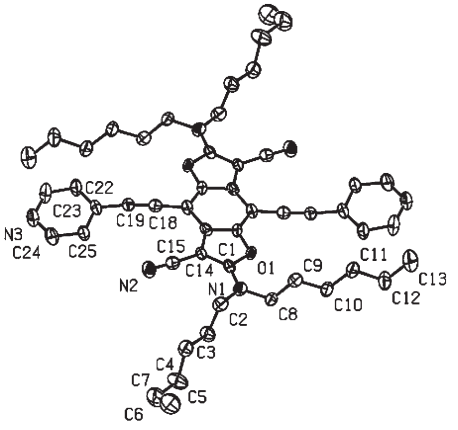

FIGURE 2. ORTEP view of molecule **A** (30% probability ellipsoids) of compound **5**. Hydrogen atoms are omitted for clarity.

extended π-conjugation. Compound **8**, however, only undergoes one irreversible reduction process, indicative of an EC mechanism, i.e., an electrochemical step followed by a fast chemical reaction step. The product of this reductive process is not clear at this point. It can therefore be deduced that the nature of the spacers plays an important role in the electrochemical properties.

The moderate onset oxidation potentials and onset reduction potentials of **7**−**9** were observed between 0.76 and 0.87 V and −(0.53−0.71) V, respectively, from which the ionization potentials (IP, HOMO levels) of 5.12−5.23 eV and electron affinities (EA, LUMO levels) of 3.65−3.83 eV were calculated according to the following equation: $E_{HOMO}/E_{LUMO} = [-(E_{onset}$ (vs Ag/AgCl) $- E_{1/2}$ (ferrocene) + 4.8)] eV, where 4.8 eV is the energy level of ferrocene below the vacuum level.[15] Again, it is worthwhile to note that electrochemical band gaps (E_g^{el} = IP − EA) of **7**−**9** are apparently varied when different spacers are incorporated into the molecular structures.

TABLE 1. Redox Potentials (*V* versus Ag/AgCl), Onset Oxidation and Reduction Potentials, Ionization Potentials (IP), Electron Affinities (EA), and Electrochemical Band Gaps E_g^{el} of Compounds 4−9

compd	$E_{1/2}^{ox1}$	$E_{1/2}^{ox2}$	$E_{1/2}^{red}$	E_{onset}^{ox1}	E_{onset}^{red}	IP[c] (eV)	EA[d] (eV)	E_g^{el} (eV)
4	0.82	1.15		0.72		−5.08		
5	0.90	1.24		0.77		−5.13		
6	0.83	1.15		0.70		−5.06		
7	0.97	1.19[a]	−0.89	0.80	−0.71	−5.16	−3.65	1.51
8	0.99	1.36	−0.72[b]	0.87	−0.63	−5.23	−3.73	1.50
9	0.93	1.25	−0.67	0.76	−0.53	−5.12	−3.83	1.29

[a]Quasi-reversible peak. [b]irreversible peak. [c]Estimated from the onset oxidation potentials using empirical equations: IP = $-(E_{onset}^{ox1} - 0.44 + 4.8)$ eV. [d]Estimated from the onset reduction potentials using empirical equations: EA = $-(E_{onset}^{red} - 0.44 + 4.8)$ eV.

Photophysics. The electronic absorption spectra of **4**−**6**, recorded in CH_2Cl_2, are shown in Figure 4. For the

(15) Chen, C. P.; Chan, S. H.; Chao, T. C.; Ting, C.; Ko, B. T. *J. Am. Chem. Soc.* **2008**, *130*, 12828.
(16) Brannon, J. H.; Magde, D. *J. Phys. Chem.* **1978**, *82*, 705.
(17) Hamai, S.; Hirayama, F. *J. Phys. Chem.* **1983**, *87*, 83.

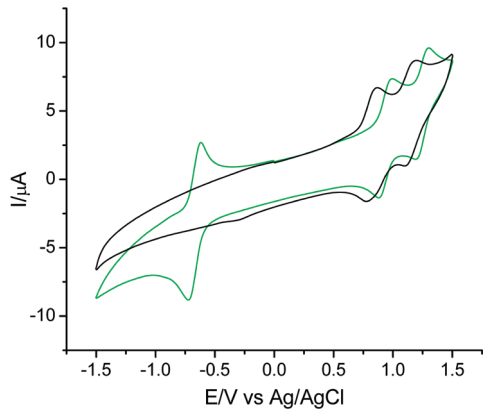

FIGURE 3. Cyclic voltammograms of **6** (black line) and **9** (green line) in CH_2Cl_2 (2×10^{-4} M); supporting electrolyte 0.1 M $(Bu_4N)PF_6$; scan rate 100 mV· s^{-1}.

molecules **5** and **6**, the most important feature is the strong ($\varepsilon \approx 2 \times 10^4$ M^{-1} cm^{-1}) and broad absorption band between 18000 cm^{-1} (555 nm) and 25000 cm^{-1} (400 nm), which peaks at around 20800 cm^{-1} (480 nm), well into the visible part of the optical spectrum, as evidenced by the intense orange-red color of both compounds. A series of further intense absorption bands is observed within the UV region of the spectrum at energies higher than 25000 cm^{-1} (400 nm). These optical absorption spectra of **5** and **6** are in stark contrast with those of other reported BDF derivatives bearing different substitution patterns, which therefore exhibit no electronic absorptions at energies lower than 25000 cm^{-1} (400 nm).[3a,12] As discussed below, this remarkable difference originates mainly from the nature of the specifically extended π-conjugated backbone of compounds **5** and **6**. In contrast, but as expected from the yellow color of compound **4**, its corresponding lowest energy absorption band is substantially blue-shifted and peaks around 25500 cm^{-1} (392 nm). This observation can be rationalized by the nonplanarity of molecule **4**, as demonstrated by its single-crystal structure. All these results clearly reflect the effect of the different spacers between the BDF core and the pyridine groups.

Furthermore, the chromophoric molecules **4**−**6** show strong fluorescence emission in CH_2Cl_2 solution at 20500 cm^{-1} (487 nm), 18800 cm^{-1} (532 nm), and 17800 cm^{-1} (562 nm) with Stokes shifts of ν_{ST} = 4950, 2000, and 3000 cm^{-1} for **4**−**6**, respectively (Figure 4 and Table 2). The corresponding luminescence quantum yields Φ_F are quite high with values > 0.75. The fluorescence excitation spectra compare well with the corresponding absorption profiles. All three compounds exhibit also a fluorescence emission in the solid state (Figure S8, Supporting Information). The solid-state emission is red-shifted with respect to the solution emission by 450, 2300, and 2000 cm^{-1} for **4**−**6**, respectively. Table 2 also includes some optical data for the strongly emitting compounds **2b** and **3**.

It is important to point out that the pyridine-substituted BDF derivatives **4**−**6** can be protonated and deprotonated under acidic and basic conditions, respectively. Upon protonation, the lowest energy absorptions are bathochromically shifted (Figure 5 for **6** and Figure S9 (Supporting Information) for **4** and **5**) due to the strong electron-withdrawing effect of the pyridinium groups. The same statement also holds true for the significant bathochromic shifts (> 5000 cm^{-1}) of the lowest energy absorptions of the corresponding methylated derivatives **7**−**9** (Table 2, Figure 5, and Figure S9 (Supporting Information)). In both cases, for protonated and methylated compounds, there is no emission observed. Taking **6** as an example, the acidic titration experiments on fluorescence intensities were performed (Figure S10, Supporting Information). Upon addition of 3 equiv of H^+, the emission is completely quenched. Upon further deprotonation, however, there is a restitution of emission. Thus, the BDF derivatives **4**−**6** can act as pH-dependent fluorescence switches. Notably, the differences between the band gap values directly measured by CV (E_g^{el} between 1.29 and 1.51 eV) and the optical band gap values obtained from UV−vis spectra (E_g^{opt} between 1.57 and 1.82 eV) lie within an acceptable range.

Computational Studies. To rationalize the electronic absorption spectra of **4**−**9**, a computational study was performed, employing density functional theory (DFT) as well as time-dependent DFT (TD-DFT) calculations with the B3LYP functional and the valence triple-ζ plus polarization (TZVP) basis set. All calculations were carried out with the TURBOMOLE V6.0 program package.[18] The ground-state optimized structures of **5**−**6** and **8**−**9**, but with NH_2 instead of $N(hexyl)_2$, were constrained to C_{2h} symmetry. In contrast, the pyridine rings in the calculated minimum-energy geometries of compounds **4** and **7** are twisted by approximately 50° with respect to the BDF core. The calculated geometries of compounds **4**−**6** are in good agreement with X-ray structures (see the Supporting Information).

The vertical TD-DFT calculations predict the $S_0 \rightarrow S_1$ electronic excitation to be an intense in-plane $\pi-\pi^*$ transition at 27920 cm^{-1} (358 nm) for **4**, at 22640 cm^{-1} (442 nm) for **5**, and at 21750 cm^{-1} (460 nm) for **6**, with oscillator strengths f_{calc} = 0.18 for **4**, 0.44 for **5**, and 0.53 for **6** (see stick spectra in Figure 4), all in fairly good agreement with the experimental data; the lowest energy absorption bands show f_{exp} = 0.20 for **4**, 0.24 for **5**, and 0.22 for **6**. This electronic transition, polarized approximately along the long molecular axis (horizontal in Figure 6), is dominated (> 90% for **4**−**6**) by the one-electron HOMO→LUMO contribution (Figure 6). This low energy electronic excitation mainly corresponds to π-electron flow from the BDF core including the substituents on the furan rings toward the pyridine groups and their spacers. This result clearly demonstrates that due to the extended π-conjugation, the HOMO−LUMO gap decreases substantially, so that the $S_0 \rightarrow S_1$ absorption for **5** and **6** is fully shifted into the visible part of the spectrum.

At higher energy, the next calculated electronic transition, $S_0 \rightarrow S_2$, at 28220 cm^{-1} (354 nm) and 26500 cm^{-1} (377 nm) for **5** and **6**, respectively, corresponds also fairly well with the experimental data (see stick spectra in Figure 4). It is dominated (> 89% for **5** and **6**) by the one-electron HOMO-1→LUMO contribution; hence, it is as well an in-plane $\pi-\pi^*$ transition in its electronic nature. Again, there occurs a substantial charge flow within the BDF skeleton and the pyridine groups through the links.

(18) (a) Ahlrich, R.; Bär, M.; Häser, M.; Horn, H.; Kölmel, C. *Chem. Phys. Lett.* **1989**, *162*, 165. (b) Bauernschmitt, R.; Ahlrich, R. *Chem. Phys. Lett.* **1996**, *256*, 454. (c) Bauernschmitt, R.; Häser, M.; Treutler, O.; Ahlrich, R. *Chem. Phys. Lett.* **1997**, *264*, 573.

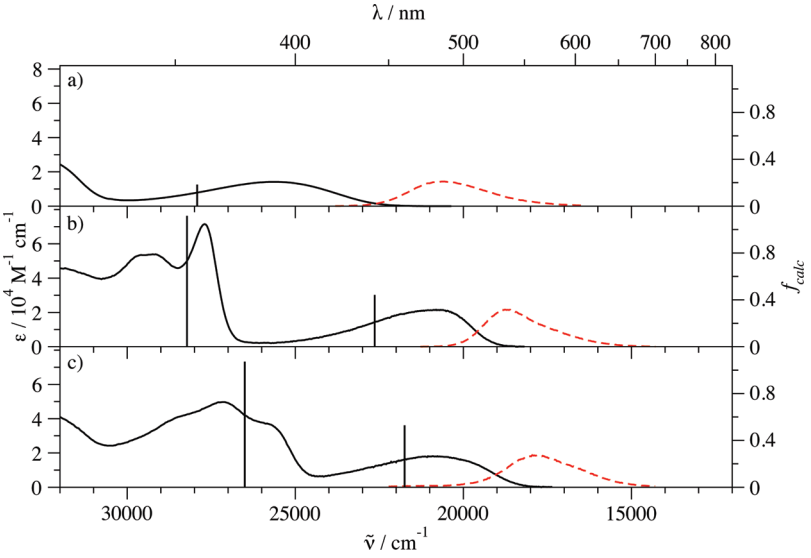

FIGURE 4. Electronic absorption (black line, 2×10^{-5} M) and fluorescence emission (red line, 2×10^{-6} M) spectra of **4** (a), **5** (b), and **6** (c) in deaerated CH_2Cl_2 solution at room temperature, together with the calculated $S_0 \rightarrow S_n$ electronic transitions.

TABLE 2. Lowest Energy Absorption and Emission Maxima A_{max} and E_{max}, Respectively, Extinction Coefficient ε, Excitation Wavelength λ_{ex}, Stokes Shift ν_{ST}, Luminescence Quantum Yield Φ_F, Optical Band Gap E_g^{opt}, and Calculated HOMO−LUMO Gaps E_g^{calc} of Compounds 2b and 3−9 in CH_2Cl_2

compd	A_{max} (cm^{-1})	ε (M^{-1} cm^{-1})	λ_{ex} (cm^{-1})	E_{max} (cm^{-1})	ν_{ST} (cm^{-1})	Φ_F	E_g^{opt} (eV)	E_g^{calc} (eV)
2b	23640	25000	22990	21640	2000	0.98[a]	2.80[c]	
3	23150	20000	22990	21280	1870	1[a]	2.74[c]	
4	25500	16000	27030	20550	4950	0.88[b]	2.80[c]	3.92
5	20800	21000	23260	18800	2000	1[a]	2.44[c]	3.14
6	20800	18000	23260	17800	3000	0.75[a]	2.35[c]	2.98
7	17400	17000					1.82[d]	2.13
8	15300	14000					1.63[d]	1.94
9	15200	15000					1.57[d]	1.94

[a]Fluorescein in 0.1 M NaOH (Φ_F = 0.95)[16] as a standard. [b]Diphenylanthracene in EtOH (Φ_F = 0.9)[17] as a standard. [c]Determined from the intersection of the absorption and emission spectra in solution. [d]Determined from the onset of the lowest energy electronic absorptions in the corresponding UV−vis spectra in solution.

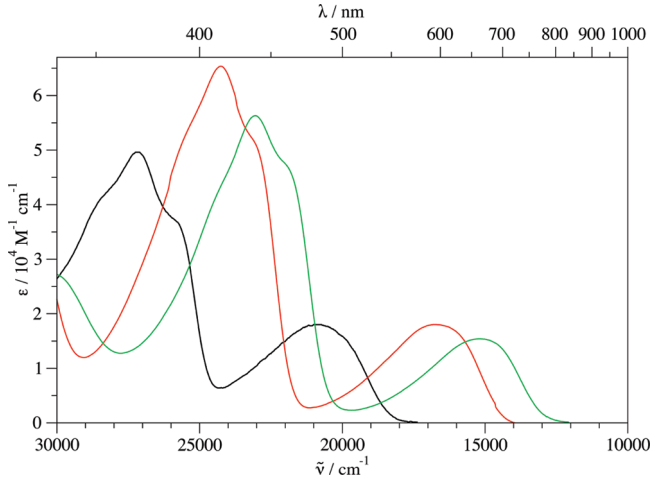

FIGURE 5. Electronic absorption spectra of **6** (black line), its protonated form (red), and its methylated form **9** (green) at room temperature.

The analogous calculations for the methylated compounds **7**−**9** (see Figures S11 and S12, Supporting Information) give similar results as discussed above for molecules **4**−**6**. As shown in Table 2, the calculated

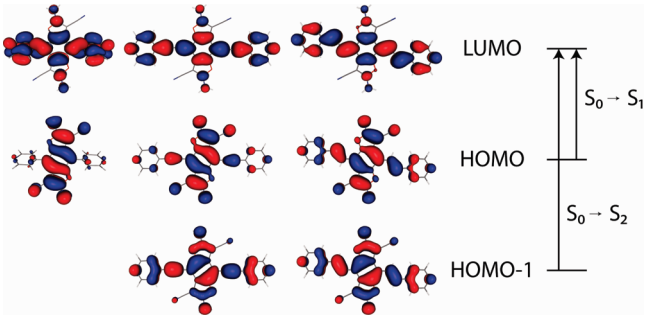

FIGURE 6. Molecular orbitals of **4** (left), **5** (middle), and **6** (right) that are involved in the $S_0 \rightarrow S_1$ (HOMO to LUMO) and $S_0 \rightarrow S_2$ (HOMO-1 to LUMO) transitions.

HOMO−LUMO gaps correspond also fairly well with the optically determined ones (E_g^{opt}).

Conclusions

We developed an efficient synthetic route to the key precursors **2a** and **2b**, which, for instance, can readily undergo Suzuki, Heck, and Sonogashira coupling reactions to afford a manifold of extended π-conjugated BDF derivatives with different functional groups and spacers in good yields.

Herein, the synthetic protocols are demonstrated with the pyridyl end-capped molecules **4**−**6**. Importantly, for these systems, a strong electronic absorption profile extends far into the visible spectral region. These are also highly luminescent materials that undergo two reversible oxidation processes. The effect of different spacers on the photophysical and electrochemical properties has been demonstrated. Moreover, upon methylation or protonation, these molecules become slightly more difficult to be oxidized and show a considerable bathochromic shift of the longest wavelength absorption band. Interestingly, they can function as pH-dependent fluorescence switches. Further studies on the construction of supramolecular systems by virtue of hydrogen bonding and metal coordination are currently in progress.

Experimental Section

Synthesis. 1,4-Diiodo-2,5-dimethoxybenzene,[19] 2,5-diiodo-1,4-benzoquinone,[20] and 1,4-dimethoxy-2,5-bis(trimethylsilylethynyl)benzene[21] were prepared according to the modified literature procedures. All chemicals and solvents were purchased from commercial sources and were used without further purification. All reactions were carried out, unless mentioned, under normal laboratory conditions in air.

Microwave reactions were conducted using the Biotage Initiator Eight EXP microwave apparatus and the corresponding vials. The reaction was performed in glass vials (capacity 5 or 20 mL) sealed with a septum, under magnetic stirring. The temperature of the reaction mixture was monitored using a calibrated infrared temperature control mounted under the reaction vial. The typical experiment was irradiated in a sealed vial at 120 °C for 30 min.

1,4-Diiodo-2,5-dimethoxybenzene. A solution of H_5IO_6 (2.92 g, 12.8 mmol) in CH_3OH (20 mL) was stirred for 10 min, and I_2 (6.38 g, 25 mmol) was added. After the solution was stirred for another 10 min, 1,4-dimethoxybenzene (2.7 g, 20 mmol) was added and the mixture heated at 70 °C for 4 h. The resulting solution was poured into a solution of $Na_2S_2O_5$ (5 g, 26 mmol) in water (50 mL). The precipitate was washed with CH_3OH and dissolved in CH_2Cl_2. After filtration, the filtrate was collected and evaporated under vacuum to afford a white crystalline product (7.02 g, 90%).

2,5-Diiodo-1,4-benzoquinone. To a solution of 1,4-diiodo-2,5-dimethoxybenzene (9.75 g, 25 mmol) in acetonitrile (180 mL) was added $(NH_4)_2Ce(NO_3)_6$ (42 g, 76 mmol). Then water (20 mL) was added to completely dissolve the oxidant. The resulting solution was stirred at rt for 30 min. After evaporation, the residue was dried, redissolved in dichloromethane, and extracted with water (3 × 50 mL). The combined organic phase was evaporated and dried under high vacuum to give an orange crystalline product (6.45 g, 70%).

1,4-Dimethoxy-2,5-bis(trimethylsilylethynyl)benzene. A mixture of 1,4-diiodo-2,5-dimethoxybenzene (1.5 g, 3.86 mmol) and $Pd(PPh_3)_2Cl_2$ (450 mg, 0.64 mmol) in DMF (10 mL) in a 20 mL vial was bubbled with N_2 for 20 min, and then CuI (350 mg, 1.8 mmol), *i*-Pr_2NH (5 mL), and trimethylsilylacetylene (1.4 g, 14 mmol) were added. The resulting mixture was subjected to microwave irradiation by prestirring for 1 min and reacted at 120 °C for 30 min. The volatile was evaporated under vacuum, and the residue was dissolved in CH_2Cl_2 (50 mL) and neutralized with 1 M HCl. The solution was extracted with CH_2Cl_2 (4 × 50 mL). The combined organic phase was evaporated by rotavapor, and the residue was subjected to column chromatography on silica gel, eluting with a mixture of hexane and CH_2Cl_2 (gradient from 0:100 to 100:0) to give a pale yellow solid (1.1 g, 86%): mp 165−167 °C; ^{1}H NMR (300 MHz, $CDCl_3$) δ 6.90 (s, 2H), 3.82 (s, 6H), 0.26 (s, 18H); ^{13}C NMR (75.4 MHz, $CDCl_3$) δ 154.2, 116.2, 113.5, 100.8, 100.4, 56.4, −0.01.

2,5-Bis(trimethylsilylethynyl)-1,4-benzoquinone. To a solution of 1,4-dimethoxy-2,5-bis(trimethylsilylethynyl)benzene (330 mg, 1 mmol) in CH_3CN (20 mL) was added $(NH_4)_2Ce(NO_3)_6$ (1.6 g, 3 mmol). Water (2 mL) was added dropwise to completely dissolve the oxidant. The resulting solution was stirred at rt for 30 min. After evaporation, the residue was dried, redissolved in CH_2Cl_2, and extracted with water (3 × 10 mL). The combined organic phase was evaporated to give a brown solid. (289 mg, 96%): mp 133−135 °C; ^{1}H NMR (300 MHz, $CDCl_3$) δ 6.87 (s, 2H), 0.25 (s, 18H); ^{13}C NMR (75.4 MHz, $CDCl_3$) δ 182.4, 137.3, 132.3, 112.4, 96.4, −0.6; HRMS, ESI (positive) calcd for $[C_{16}H_{20}O_2Si_2Na]^+$ 323.0894, found 323.0902.

2,6-Diamino-4,8-diethynylbenzo[1,2-*b*:4,5-*b*′]difuran-3,7-dicarbonitrile (1b). 2,5-Bis(trimethylsilylethynyl)-1,4-benzoquinone (280 mg, 0.9 mmol) and malononitrile (200 mg, 3 mmol) were dissolved in THF (50 mL), and then Bu_4NF (1 g, 3.2 mmol) was added. The mixture was stirred at rt for 0.5 h and poured into water (50 mL). The resulting mixture was extracted with CH_2Cl_2 (4 × 50 mL). The combined organic phase was evaporated and washed with hexane and diethyl ether to give a brown microcrystalline product (30 mg, 11%): mp 233−235 °C; ^{1}H NMR (300 MHz, DMSO-d_6) δ 8.42 (s, 4H), 4.84 (s, 2H); ^{13}C NMR (75.4 MHz, DMSO-d_6) δ 166.6, 145.3, 122.3, 114.1, 94.5, 91.2, 73.4, 61.2; HRMS, ESI (positive) calcd for $[C_{16}H_{17}N_4O_2]^+$ 287.0569, found 287.0560.

2,6-Diamino-4,8-diiodobenzo[1,2-*b*:4,5-*b*′]difuran-3,7-dicarbonitrile (1a). To a solution of 1,4-diiodoquinone (2 g, 5.55 mmol) and malononitrile (990 mg, 15 mmol) in methanol (50 mL) was added piperidine (4 mL). The mixture was stirred for 1 h at 60 °C. A brown precipitate was formed. After centrifugation, the solid was washed with methanol (2 × 10 mL) and dried to give a brown powder (1.24 g, 45%): mp 240 °C dec; ^{1}H NMR (300 MHz, $CDCl_3$) δ 8.36 (s, 4H); ^{13}C NMR (75.4 MHz, $CDCl_3$) δ 166.6, 144.8, 122.8, 114.8, 64.1, 62.7; HRMS (EI) calcd for $[C_{12}H_4N_4O_2I_2]$ 489.8424, found 489.8424.

Compound 2a. To a solution of **1a** (300 mg 0.61 mmol) in DMF (20 mL) were added 1-bromohexane (2.5 mL, 17.5 mmol) and K_2CO_3 (3 g, 21.75 mmol). The resultant mixture was heated at 90 °C for 1.5 h, poured into water (50 mL), and extracted with CH_2Cl_2 for (3 × 50 mL). The combined organic phase was concentrated to the volume of 2 mL, precipitated with the addition of methanol, and centrifuged to give a pale yellow solid (260 mg, 50%): mp 148−150 °C; ^{1}H NMR (300 MHz, $CDCl_3$) δ 3.58 (t, J = 7.2 Hz, 8H), 1.73 (m, 8H), 1.35 (m, 24H), 0.89 (t, J = 7.0 Hz, 12H); ^{13}C NMR (75.4 MHz, $CDCl_3$) δ 163.0, 145.1, 123.5, 116.5, 65.1, 61.3, 50.2, 31.5, 28.4, 26.1, 22.6, 14.0; HRMS, ESI (positive) calcd for $[C_{36}H_{53}N_4O_2I_2]^+$ 827.2252, found 827.2258.

Compound 3. A mixture of **2a** (826 mg, 1 mmol), $Pd(PPh_3)_2Cl_2$ (175 mg, 0.25 mmol), CuI (50 mg, 0.26 mmol), and piperidine (4 mL) in triethylamine (30 mL) was bubbled with N_2 for 10 min, and then trimethylsilylacetylene (600 mg, 6 mmol) was added. The resulting solution was heated at 110 °C overnight in an inert atmosphere. The volatile was evaporated by rotavapor, and the residue was subjected to column chromatography on silica gel, eluting initially with hexane and then with 1:1 hexane/CH_2Cl_2 to yield a yellow crystalline product (500 mg, 65%): mp 160−162 °C; ^{1}H NMR (300 MHz, $CDCl_3$) δ 3.57 (t, J = 7.5 Hz, 8H), 1.71 (m, 8H), 1.33 (m, 24H), 0.88 (t, J = 6.9 Hz, 12H), 0.28

(19) Zhang, J.; Cui, Y.; Wang, M.; Liu, J. *Chem. Commun.* **2002**, 2526.
(20) López-Alvarado, P.; Avendaño, C.; Menéndez, J. C. *Synth. Commun.* **2002**, *32*, 3233.
(21) Dirk, S. M.; Price, D. W.; Chanteau, S.; Kosynkin, D. V.; Tour, J. M. *Tetrahedron* **2001**, *57*, 5109.

(s, 18H); ^{13}C NMR (75.4 MHz, $CDCl_3$) δ 163.0, 145.7, 123.2, 115.8, 106.3, 96.1, 93.8, 62.6, 50.1, 31.5, 28.5, 26.2, 22.6, 14.0, −0.40; HRMS, ESI (positive) calcd for $[C_{46}H_{71}N_4O_2Si_2]^+$ 767.5110, found 767.5132.

Compound 2b. To a solution of **3** (460 mg, 0.6 mmol) in THF (15 mL) was added $Bu_4NF\cdot 3H_2O$ (1 g, 3.2 mmol). The mixture was stirred at rt for 30 min and then poured into water (50 mL) and extracted with CH_2Cl_2 (3 × 50 mL). The solvent was removed under high vacuum to give a pale yellow solid (240 mg, 64%): mp 123−125 °C; ^{1}H NMR (300 MHz, $CDCl_3$) δ 3.65 (s, 2H), 3.58 (t, J = 7.5 Hz, 8H), 1.72 (m, 8H), 1.34 (m, 24H), 0.89 (t, J = 6.8 Hz, 12H); ^{13}C NMR (75.4 MHz, $CDCl_3$) δ 163.1, 145.7, 123.5, 115.9, 95.3, 88.1, 73.0, 62.5, 49.9, 31.4, 28.4, 26.1, 22.5, 14.0; HRMS, ESI (positive) calcd for $[C_{40}H_{55}N_4O_2]^+$ 623.4320, found 623.4334.

Compound 4. A mixture of compound **2a** (240 mg, 0.3 mmol), 4-pyridylboronic acid (120 mg, 1 mmol), $Pd(PPh_3)_2Cl_2$ (40 mg, 0.06 mmol), and Cs_2CO_3 (200 mg, 0.62 mmol) was added to a 5 mL microwave vial. The reactor was sealed, evacuated, and purged with N_2. Then DMF (2.5 mL) and water (0.5 mL) were successively added. The reactor was subjected to microwave irradiation at 120 °C for 30 min. The resulting mixture was poured into water (10 mL) and extracted with CH_2Cl_2 (20 mL). The volatile was evaporated by rotavapor, and the residue was subjected to column chromatography on neutral alumina, eluting with 100:5 CH_2Cl_2/triethylamine, to afford a yellow solid product (180 mg, 85%): mp 92−94 °C; ^{1}H NMR (300 MHz, $CDCl_3$) δ 8.77 (d, J = 6.0 Hz, 4H), 7.51 (d, J = 6.0 Hz, 4H), 3.45 (t, J = 7.5 Hz, 8H), 1.64 (m, 8H), 1.26 (m, 24H), 0.88 (t, J = 6.4 Hz, 12H); ^{13}C NMR (75.4 MHz, $CDCl_3$) δ 163.7, 149.5, 142.9, 139.2, 125.1, 120.7, 116.3, 112.1, 61.2, 50.1, 31.5, 28.5, 26.1, 22.5, 13.9; HRMS, ESI (positive) calcd for $[C_{46}H_{61}N_6O_2]^+$ 729.4851, found 729.4857.

Compound 5. A mixture of **2a** (164 mg, 0.2 mmol), 4-ethynylpyridine (80 mg, 0.77 mmol), $Pd(PPh_3)_2Cl_2$ (40 mg, 0.06 mmol), CuI (10 mg 0.05 mmol), and piperidine (2 mL) in triethylamine (20 mL) was bubbled with N_2 for 10 min, and then the resulting solution was heated at 110 °C overnight in an inert atmosphere. The volatile was evaporated by rotavapor, and the residue was subjected to column chromatography on neutral alumina, eluting with a mixture of CH_2Cl_2 and 1% triethylamine to afford an orange crystalline product (100 mg, 65%): mp 224−226 °C; ^{1}H NMR (300 MHz, $CDCl_3$) δ 8.61(d, J = 5.0 Hz, 4H), 7.51 (d, J = 5.4 Hz, 4H), 3.64 (t, J = 7.5 Hz, 8H), 1.78 (m, 8H), 1.36 (m, 24H), 0.88(t, J = 6.8 Hz, 12H); ^{13}C NMR (75.4 MHz, $CDCl_3$) δ 163.1, 149.8, 145.2, 130.9, 125.2, 123.9, 116.2, 97.2, 95.7, 62.6, 50.3, 31.5, 28.5, 26.2, 22.6, 14.0; HRMS, ESI (positive) calcd for $[C_{50}H_{61}N_6O_2]^+$ 777.4851, found 777.4872.

An alternative synthetic route to **5**: A mixture of **2b** (124 mg, 0.2 mmol), 4-iodopyridine (160 mg, 0.8 mmol), $Pd(PPh_3)_2Cl_2$ (28 mg, 0.04 mmol), and CuI (10 mg, 0.05 mmol) in triethylamine (20 mL) was bubbled with N_2 for 10 min, and then the mixture was heated at 110 °C in an inert atmosphere overnight. The volatile was evaporated by rotavapor, and the residue was subjected to column chromatography on neutral alumina, eluting with a mixture of CH_2Cl_2 and 1% triethylamine to afford an orange crystalline product (45 mg, 29%).

Compound 6. A mixture of **2a** (164 mg, 0.2 mmol), 4-vinylpyridine (90 mg, 0.86 mmol), $Pd(PPh_3)_2Cl_2$ (40 mg, 0.06 mmol), and Cs_2CO_3 (200 mg, 0.62 mmol) in dioxane (10 mL) was bubbled with N_2 for 10 min, and then the resulting solution was heated at 110 °C in an inert atmosphere overnight. The volatile was evaporated by rotavapor, and the residue was subjected to column chromatography on silica gel, eluting with CH_2Cl_2 to afford a red crystalline product (97 mg, 62%): mp 222−224 °C; ^{1}H NMR (300 Mz, $CDCl_3$) δ 8.59 (d, J = 6.0 Hz, 4H), 8.21 (d, J = 16.4 Hz, 4H), 7.40−7.35 (m, 6H), 3.63 (t, J = 7.6 Hz, 8H), 1.80 (m, 8H) 1.34 (m, 24H), 0.88 (t, J = 6.8 Hz, 12H); ^{13}C NMR (75.4 MHz, $CDCl_3$) δ 163.2, 150.4, 144.9, 142.9, 130.6, 123.2, 122.6, 120.8, 118.7, 110.4, 61.3, 50.7, 31.6, 28.7, 26.4, 22.6, 14.0; HRMS, ESI (positive) calcd for $[C_{50}H_{65}N_6O_2]^+$ 781.5164, found 781.5187.

Compound 7. A mixture of compound **4** (30 mg, 0.04 mmol) and iodomethane (70 mg, 0.5 mmol) in acetonitrile (4 mL) was treated under microwave irradiation (120 °C, 30 min). The resulting purple solution was poured into saturated KPF_6 aqueous solution (10 mL), and a purple precipitate immediately formed. The suspension was centrifuged, and then the precipitate was washed with water 3 times and redissolved in acetonitrile. After filtration, the filtrate was evaporated by rotavapor and dried in vacuum to give a purple solid product (28 mg, 65%): mp 154−156 °C; ^{1}H NMR (300 MHz, CD_3CN) δ 8.76 (d, J = 6.4 Hz, 4H), 8.25 (d, J = 6.4 Hz, 4H), 4.37 (s, 6H), 3.54 (t, J = 7.3 Hz, 8H), 1.67 (m, 8H), 1.28 (m, 24H), 0.88 (t, J = 6.2 Hz, 12H); ^{13}C NMR (75.4 MHz, CD_3CN) δ 165.0, 148.4, 145.6, 143.7, 130.1, 122.1, 110.6, 61.5, 50.9, 49.2, 32.1, 28.8, 26.6, 23.2, 14.2 ; HRMS, ESI (positive) calcd for $[C_{48}H_{66}N_6O_2]^{2+}$ 379.2618, found 379.2627.

Compound 8. A mixture of compound **5** (35 mg, 0.046 mmol) and iodomethane (30 mg, 0.21 mmol) in acetonitrile (4 mL) was treated under microwave irradiation (120 °C, 30 min). The resulting blue solution was poured into saturated KPF_6 aqueous solution (10 mL), and a blue precipitate formed immediately. The suspension was centrifuged, and then the precipitate was washed with water for 3 times and redissolved in acetonitrile. After filtration, the filtrate was evaporated by rotavapor and dried in vacuum to give a blue crystalline product (36 mg, 73%): mp 232−234 °C; ^{1}H NMR (300 MHz, CD_3CN) δ 8.61 (d, J = 6.6 Hz, 4H), 8.09 (d, J = 6.6 Hz, 4H), 4.28 (s, 6H), 3.71 (t, J = 7.2 Hz, 8H), 1.78 (m, 8H), 1.38 (m, 24H), 0.91 (t, J = 7.0 Hz, 12H); ^{13}C NMR (75.4 MHz, CD_3CN) δ 164.5, 146.3, 146.2, 140.0, 129.7, 125.9, 117.0, 96.1, 95.6, 94.0, 62.9, 50.9, 49.2, 32.1, 28.9, 26.7, 23.2, 14.2; HRMS, ESI (positive) calcd for $[C_{52}H_{66}N_6O_2]^{2+}$ 403.2618, found 403.2636.

Compound 9. A mixture of compound **6** (25 mg, 0.032 mmol) and iodomethane (70 mg, 0.5 mmol) in acetonitrile (4 mL) was treated under microwave irradiation (120 °C, 30 min). The resulting purple solution was poured into saturated KPF_6 aqueous solution (10 mL), and a dark-green precipitate formed immediately. The suspension was centrifuged, and then the precipitate was washed with water 3 times and redissolved in acetonitrile. After filtration, the filtrate was evaporated by rotavapor and dried in vacuum to give a dark-green powder product (26 mg, 73%): mp 195−197 °C; ^{1}H NMR (300 MHz, CD_3CN) δ 8.50 (m, 6H), 7.94 (d, J = 6.6 Hz, 4H), 7.60 (d, J = 16.4 Hz, 2H), 4.22 (s, 6H), 3.69 (t, J = 7.5 Hz, 8H), 1.80 (m, 8H), 1.32 (m, 24H), 0.87 (t, J = 6.8 Hz, 12H); ^{13}C NMR (75.4 MHz, CD_3CN) δ 164.5, 154.1, 146.1, 144.0, 131.3, 128.5, 124.7, 119.3, 111.3, 61.8, 51.3, 48.4, 32.2, 29.0, 26.8, 23.2, 14.2; HRMS, ESI (positive) calcd for $[C_{52}H_{70}N_6O_2]^{2+}$ 405.2775, found 405.2788.

Acknowledgment. This work was supported by the Swiss National Science Foundation (Grant No. 200020-116003 and 200020-130266/1) and EU (FUNMOLS FP7-212942-1).

Supporting Information Available: General experimental methods and ^{1}H spectra for all new compounds, the solid state emission spectra of **4**−**6**, additional absorption spectra, computational studies of **7**−**9**, calculated triplet energies for **6**, CIF files for **1b** and **4**−**6** (CCDC 752868, 773634, 745180, 745181); molecular structures of **1b**, **4**, and **6**; crystal packing diagrams of **1b** and **4**−**6**. This material is available free of charge via the Internet at http://pubs.acs.org.